Asian Journal of Chemistry; Vol. 35, No. 7 (2023), 1741-1748

ASIAN JOURNAL OF CHEMISTRY

https://doi.org/10.14233/ajchem.2023.27872

Synthesis of *Annona glabra* Mediated Silver Nanoparticles, their Photocatalysis and Toxicity on *Daphnia magna*

S.R. WICKRAMARACHCHI[1,*], Y.L. PARAGODAARACHCHI[2], C.R. DE SILVA[3], A.D.L.C. PERERA[4] and L.D. AMARASINGHE[5]

[1]Department of Chemistry, University of Kelaniya, Kelaniya, Sri Lanka
[2]Postgraduate Institute of Science, University of Peradeniya, Peradeniya, Sri Lanka
[3]Department of Chemistry & Physics, Western Carolina University, Cullowhee, NC 28723, U.S.A.
[4]Department of Chemistry, University of Peradeniya, Peradeniya, Sri Lanka
[5]Department of Zoology & Environmental Management, University of Kelaniya, Kelaniya, Sri Lanka

*Corresponding author: Fax: +94 112 903203; Tel: +94 112 903253; E-mail: suranga@kln.ac.lk

Received: 7 April 2023; *Accepted*: 13 June 2023; *Published online*: 6 July 2023; AJC-21301

This work reports the synthesis of silver nanoparticles (AgNPs) using the leaf extract of *Annona glabra* as a green synthetic route and assessment of its photocatalytic property using methelyne blue as a model dye and toxic effect against an aquatic model, *Daphnia magna*. Leaf extract prepared at 100 ºC, 1% plant extract, 1 mM of $AgNO_3$, 3 h incubation time were optimized for the synthesis of AgNPs. Surface plasmon resonance peak of AgNPs laid around 419 nm. Spherical nanoparticles were in the size ranges 50-80 and 110-195 nm. Biomolecules were present as capping agents on AgNPs. AgNPs have cubic face centered lattice structure and the average particle size as calculated using Debye-Scherrer formula is 55 nm. Green synthesized AgNPs reduced the absorbance of methelyne blue dye by 89% in 3 h showing prominent photocatalytic activity. The EC_{50} of AgNPs was found to be 1.78 ± 0.20 mg/L against *Daphnia magna* showing a lower toxicity than silver ions.

Keywords: Green synthesis, Silver nanoparticles, *Annona glabra*, *Daphnia magna*, Photocatalysis.

INTRODUCTION

Nanotechnology deals with particles that have sizes in the range of 1-100 nm. Due to the small size of these particles, the surface area to volume ratio is high providing them with unique properties from their bulk equivalents [1]. Nanoparticles and nanomaterials constitute an active area of research and because of the tunable physiological properties of nanoparticles, like melting point, electrical and thermal conductivity, catalytic activity and light absorption, they have gained prominence in technological advancements [2]. These nanomaterials show a possibility to solve the main challenges faced in the areas of solar energy conversion, biomedical science, water treatment and catalysis thus there is an increasing demand for nanomaterials. Synthesis of silver nanoparticles (AgNPs) is also easier which can be conducted at room temperature using physical, chemical and biological processes. The chemical methods used to synthesize AgNPs involve the use of reducing agents and stabilizing agents which subsequently pose a risk to the environment. For these reasons, green synthesis of AgNPs is a major area of interest. Among the variety of biological methods, use of plant extracts is more popular due to ease of handling and low cost. Various biomolecules present in plant extracts serve as reducing agents of Ag^+ and stabilizing agents of formed AgNPs. Plant leaves are commonly used for nanoparticle synthesis and among the wide range of plants *Mangifera indica* and *Azadirachta indica* have commonly used [3,4].

In this study, we use the leaf extract of *Anonna glabra* to fabricate AgNPs following our previous attempt using the same plant extract [5]. Remarkable properties and behaviour of AgNPs are the reason behind the intensive use of AgNPs in fields like electronics, appliances, textile and medical applications. AgNPs have the ability to absorb visible and UV light due to their surface plasmon resonance (SPR) and due to intra-band transition between 4*d* and 5*sp* bands [6]. AgNPs can therefore be considered a catalyst that utilize full solar spectrum. AgNPs with

smaller sizes have shown to be more efficient in degradation of the dyes than the larger particles. This is due to the higher surface area available, which cause faster electron transport to break bonds in the dyes.

Furthermore, larvicidal toxicity of the *A. glabra* mediated AgNPs on dengue vector mosquito larvae is reported recently [5]. Such applications of nanoparticles can ultimately pose a threat to aquatic organisms. AgNPs can exert toxic effects in cellular environment in two ways; by the production of reactive oxygen species and by release of Ag^+ ions, which can denature biomolecules like proteins. Reactive oxygen species, such as hydrogen peroxide, can cause cell death through direct or indirect interaction with intracellular macromolecules, such as DNA, lipids and proteins [7]. The toxic effects of AgNPs on fish is caused by interaction of Ag^+ ions with gills inhibiting basolateral Na^+, K^+-ATPase activity. This ultimately causes issues in osmoregulation of fish by inhibiting active Na^+ and Cl^- uptake, due to disruption of this enzyme [8]. AgNPs are shown to cause genomic damage and instability in Zebrafish [9]. The toxicity of AgNPs towards three aquatic invertebrates from different trophic levels have been studied by Lekamge *et al.* [10]. The toxicity of AgNPs varies in the order of *Daphnia carinata* > *Paratya australiensis* > *Hydra vulgari* [10]. Present study aims at analyzing the photocatalytic activity and the toxic potential of *A. glabra* mediated AgNPs against *Daphnia magna*. In the previous attempt of biofabrication of AgNPs using *Annona glabra* by our research group, AgNPs were synthesized under ambient temperature and light [5]. In this study, AgNPs were synthesized under dark conditions to obtain more control over particle size. Furthermore, stabilization studies of AgNPs was also conducted in order to enhance their properties.

EXPERIMENTAL

Annona glabra leaves were collected from the locality of University of Kelaniya. Silver nitrate (*m.w.* 169.87 g/mol with > 99% assay) and anhydrous methylene blue (*m.w.* 319.85 g/mol) were purchased from Sigma-Aldrich, USA. *Daphnia magna* was collected from a culture center in Kaluthara, Sri Lanka.

Preparation of plant leaf extract: *A. glabra* leaf extract was made by following the method given by Amarasinghe *et al.* [5]. Briefly, cleaned chopped fresh leaves (20 g) were heated with deionized water (100.0 mL) for 1 h. The extraction temperature was changed (60-100 °C) to obtain the optimum amount of biomaterials in the extract for the synthesis of NPs. Supernatant was separated by filtration after cooling the extract to room temperature. Leaf extract solution was refrigerated until further use.

Synthesis of AgNPs: The method given by Amarasinghe *et al.* [5] was used for the synthesis of AgNPs with slight modifications. In this study, dark conditions were used to slow down the synthesis rate in order to avoid the aggregation of synthesized AgNPs. A secondary stabilization of synthesized AgNPs was conducted using Tween-80 solution (1%, 20.0 mL) by continous stirring for 3 h. The solution was centrifuged at 600 rpm for 20 min and then the pellet was freeze dried to obtain dry AgNPs.

Characterization

UV-visible spectrometry: Ultrasonicated samples of AgNPs were scanned between 200 nm to 800 nm at a resolution of 1 nm at room temperature using Shimadzu UV-Vis spectrophotometer (UV-1800). Quartz cuvette with 1 cm path length was used.

Particle size measurements: Particle size was determined by DLS using the CILAS NANO DS particle size analyzer.

Electron microscopic analysis: TEM analysis was performed using TEM-H9500 microscope with an operating voltage of 300 kV. A dispersion of nanoparticles (1 mg/mL) was made in nanopure water and was drop casted 20 µL) onto a carbon coated copper grid (300 mesh). Samples were dried at room temperature for 4 h. SEM analysis was performed using STEM-Hitachi HD2000 microscope with an operating voltage of 200 kV. Samples were treated in the same manner as for TEM analysis.

Fourier transform infrared (FTIR) analysis: The FTIR measurement was performed on FTIR spectrometer (Perkin Elmer, Spectrum two) with the help of attenuated total reflection (ATR) attachment. The spectra were obtained in the range of 4000-750 cm^{-1}.

X-ray diffraction analysis: The X-ray diffraction analysis was done using Siemens D5000 powder X-ray diffractometer.

Photocatalytic activity: Photocatalytic activity of the synthesized AgNPs was tested under air atmosphere in the presence of sunlight using methylene blue dye as described by Vanaja *et al.* [11]. Dye solution (1×10^{-5} M) was mixed with AgNPs (25 mg/mL, 2.0 mL) and the solution was placed in the dark for 30 min under continuous stirring to establish the absorption/desorption equilibrium between the dye and AgNPs. The solution was then exposed to sunlight with slow agitation. At 30 min intervals, 4 mL aliquots were collected and centrifuged at 6000 rpm for 5 min. The supernatant was analyzed using UV-visible spectrophotometer. The test was conducted for 3 h. The photocatalytic activities of both bare and stabilized AgNPs were also assessed using the method given above.

Toxicity analysis-acute immobilization test with *Daphnia magna*: Acute toxicity test for *D. magna* was conducted at 27-28 ºC according to the OECD guideline 202 (OECD, 2004) [12]. Young daphnids aged less than 24 h (neonates) derived from a healthy stock (*i.e.* showing no signs of stress such as high mortality, discoloured animals, *etc.*) were used in the toxicity tests. Test solutions of AgNPs with concentrations ranging from (0.01-5 mg/L) and Ag^+ (0.5-2 µg/L) were used. Sterile plastic containers were used as the test vessels. Test vessels were filled with 20 mL of dilution water or test metal solutions. Ratio of air/water volume in the vessels were identical for test and control groups. Twenty young daphnids, divided into four groups of five animals each, were used at each test concentration and for the controls. The test was conducted using a static system. The test vessels were not aerated during the test. The neonates were not fed during the test. Test vessels were covered using a mesh to avoid entry of dust into the test vessels. Each test vessel was checked for immobilized daphnids 48 h after the beginning of the test. Immobility was evaluated

by observing the movement of daphnids 15 s after the gentle agitation of the medium. In addition to immobility, any abnormal behaviour or appearance also were reported.

RESULTS AND DISCUSSION

Formation of AgNPs from *Annona glabra* leaves were visually monitored by the colour change of solution from faint yellow to reddish brown and confirmed by the SPR band positioned at 417 nm in the UV-visible spectra of AgNPs (Fig. 1a). Moreover, Fig. 1b displays the particle size distribution of the biosynthesized AgNPs using *A. glabra* extract. The nanoparticles are polydispersed, with 50% having a diameter of less than 191.8 nm.

Effect of extraction temperature of plant extract on the synthesis of AgNPs: Fig. 2 illustrates the UV-visible absorption spectra and particle size of AgNPs prepared by varying extraction temperature of the leaf extract, respectively. No regular pattern is observed in the position of SPR peak with increasing temperature. For leaf extracts made at 60, 70 and 100 ºC, SPR peaks were positioned around the characteristic range (400-450 nm) of AgNPs. However, a deviation was observed in the λ_{max} of SPR peaks obtained for AgNPs, prepared with plant extracts made at 80 and 90 ºC. Their SPR peak was positioned below 400 nm (Fig. 2). These AgNPs do not show the characteristic SPR band of AgNPs. The deviation in λ_{max} from the normal value of SPR band of AgNPS, at 80 and 90 ºC is also reflected in their DLS measurements (Fig. 2b). AgNPs formed at 80 and 90 ºC have a significantly larger size than that of others. Hence, this deviation in λ_{max} from the characteristic value of SPR band of AgNPs can be attributed to the larger size of nanoparticles formed at higher temperature. However, contradicting this trend, we obtained the smallest AgNPs at 100 ºC (Table-1). Further studies are needed to explain the reason for this phenomenon.

A study conducted using *Zingiber officinale* to investigate the effect of temperature and other conditions on the extraction of flavonoids and phenolic compounds (help in formation and stabilization of AgNPs), has found that higher temperatures

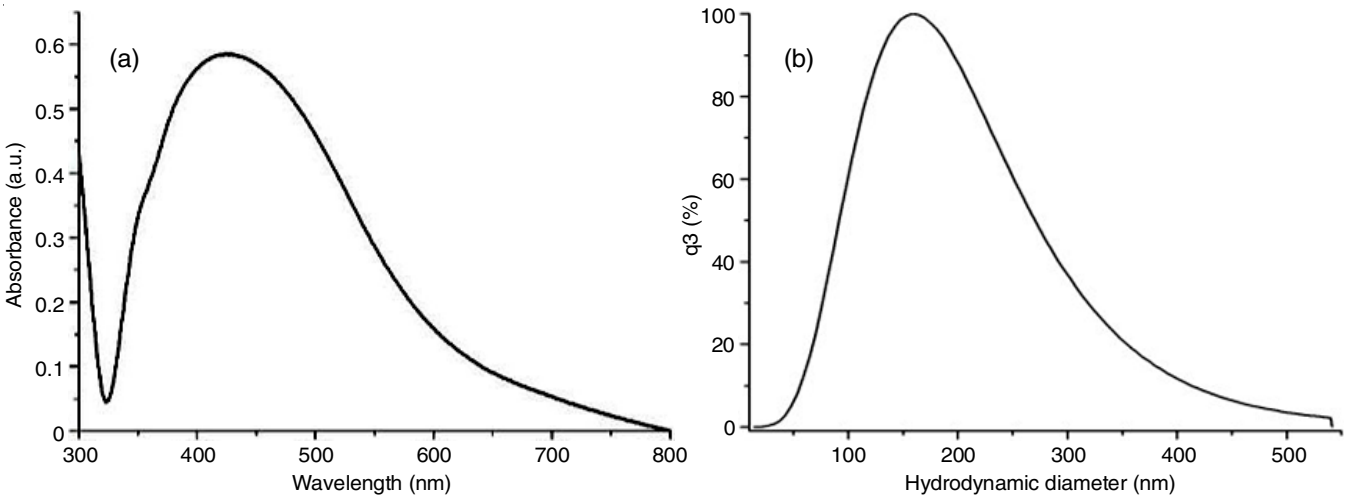

Fig. 1. UV-visible spectrum showing the SPR band (a) and the size distribution (b) of synthesized AgNPs using 5 mM $AgNO_3$ and 10% (v/v) plant extract

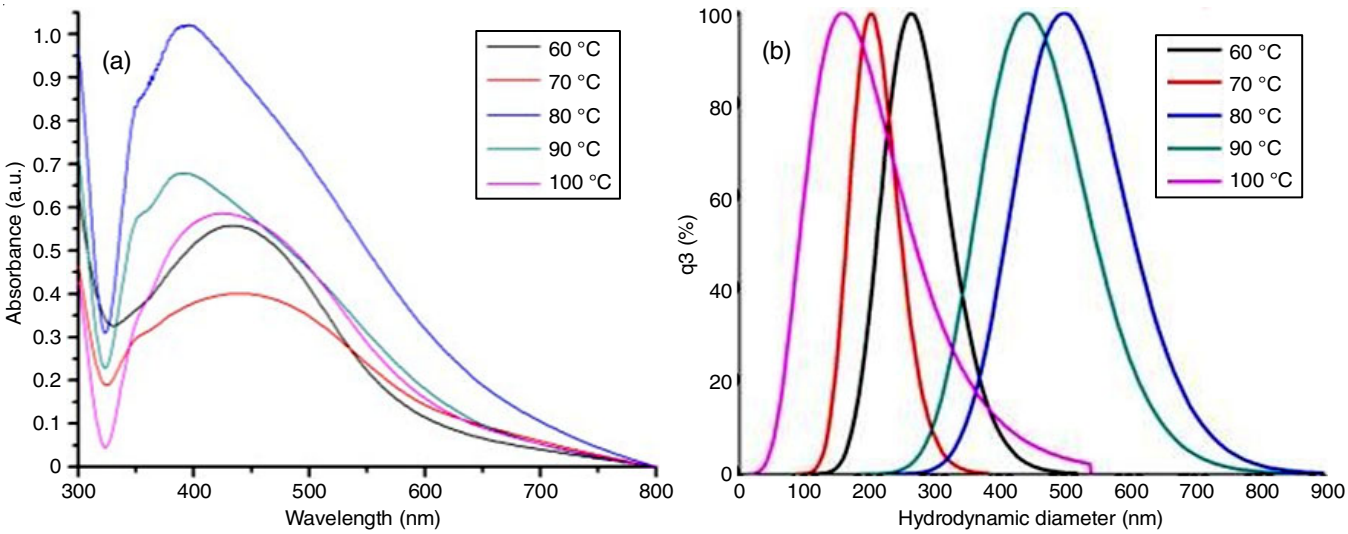

Fig. 2. SPR bands (a) and the size distribution (b) of synthesized AgNPs using plant extracts prepared at varying temperatures (10% plant extract, 5 mM $AgNO_3$ solution, 3 h incubation time)

TABLE-1
POSITION OF THE SPR PEAK AND THE PARTICLE SIZE AT DIFFERENT EXTRACTION TEMPERATURES OF THE PLANT EXTRACT

Temperature (°C)	λ_{max} (nm)	Average particle size (nm)
60	443	269
70	438	206
80	397	508
90	398	451
100	427	191

TABLE-2
POSITION OF THE SPR PEAK AND THE PARTICLE SIZE AT DIFFERENT CONCENTRATIONS OF THE PLANT EXTRACT

Concentration of plant extract (%)	λ_{max} (nm)	Average particle size (nm)
10	445	206
20	471	318
30	< 400	–
40	< 400	–
50	< 400	–

helped in extraction of higher amounts of flavonoids and phenolic compounds [13]. Several phytochemicals involved in the synthesis and stabilization of AgNPs may have been extracted at 100 ºC. According to these results, leaf extracts prepared at 60, 70 and 100 ºC can be used to synthesize AgNPs. As AgNPs with smaller size is more suitable for different applications, due to higher surface area to volume ratio, plant extract prepared at 100 ºC was chosen for further studies.

Effect of plant extract concentration: The SPR band of the UV-visible spectrum of AgNPs was monitored while changing the concentration of plant extract used (Fig. 3). Absorbance and the λ_{max} of the SPR band increased when the plant extract was increased from 10% to 20%. The absorbance increased due to the higher amount of nanoparticles formed at higher plant concentration whereas the bathochromic shift in λ_{max} can be attributed to the increase in the size of AgNPs formed [4]. The λ_{max} of the SPR peak for 10% plant extract is positioned at 445 nm and the average particle size was 206 nm whereas for 20% solution, it is positioned at 471 nm and the average particle size was 318 nm (Fig. 3). The SPR peak fades away and a new peak appears below 400 nm at plant extract concentrations ≥ 30% indicating the deviation of AgNPs from the nano range. Higher amounts of plant extract cause more abrupt nucleation and faster growth while producing small aggregates. This is evidenced by the DLS measurements showing increasing particle sizes at higher plant extract concentrations.

Effect of $AgNO_3$ concentration: Table-3 illustrates the effect of varying the concentration of $AgNO_3$ on the nanoparticle synthesis. The SPR band shifts when the $AgNO_3$ concentration is varied (Fig. 4a-b). A redshift of the peaks from 424 nm to 463 nm is observed with increasing $AgNO_3$ concentration. The DLS measurements show a parallel shift towards larger particle size with increasing $AgNO_3$ concentration (Fig. 4b). An increase in the particle size with the increase of precursor concentration is due to the agglomeration of formed AgNPs. The SPR peak intensity increases with increasing $AgNO_3$ concentration indicating the formation of higher amount of AgNPs. The smallest particle size (183 nm) was obtained for AgNPs prepared using 1 mM $AgNO_3$ solution. The SPR band diminished at 20 mM $AgNO_3$ indicating a deviation from nano range. Due to the higher concentration of the precursor, the rate of formation of AgNPs could be high, which ultimately cause aggregation of the nanoparticles. This is further evidenced by the sudden increase of the size of nanoparticles formed at this concentration (Table-3). In a study, where AgNPs were synthesized using *Prunus persica* leaves, varying $AgNO_3$ concentration has increased the absorption of the SPR peak up to 2 mM and then the absorbance

TABLE-3
POSITION OF THE SPR PEAK AND THE PARTICLE SIZE AT DIFFERENT CONCENTRATIONS OF $AgNO_3$

$AgNO_3$ concentration (mM)	λ_{max} (nm)	Average particle size (nm)
1	424	183
5	438	206
10	461	315
20	463	571

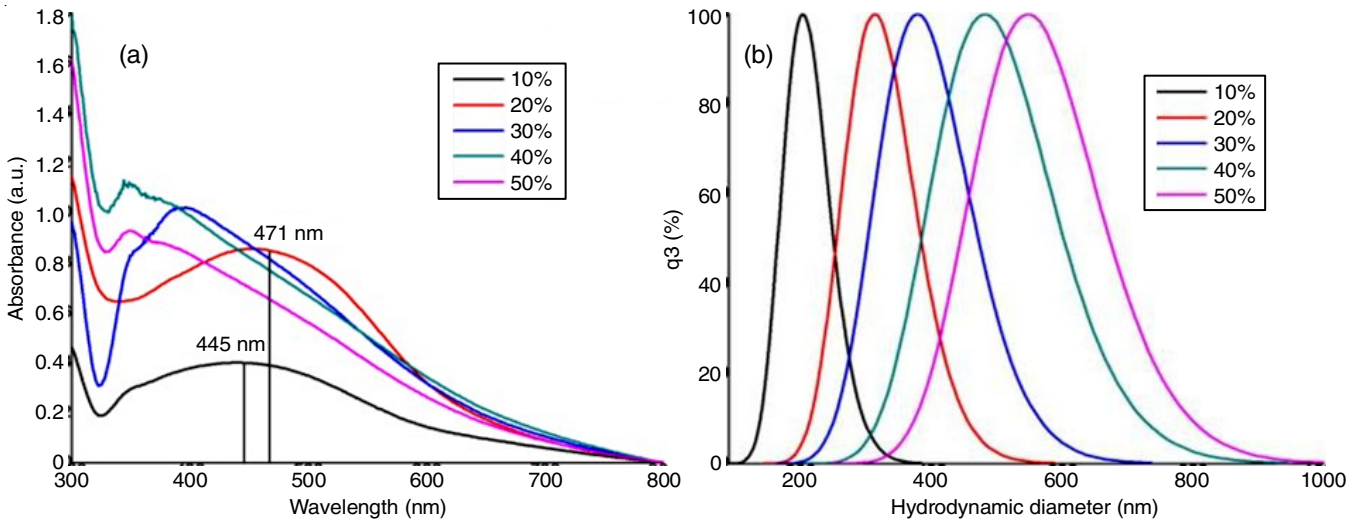

Fig. 3. SPR band (a) and size distribution (b) of AgNPs formed at various concentrations of plant extract (5 mM $AgNO_3$ solution, 100 °C extraction temperature, 3 h incubation time)

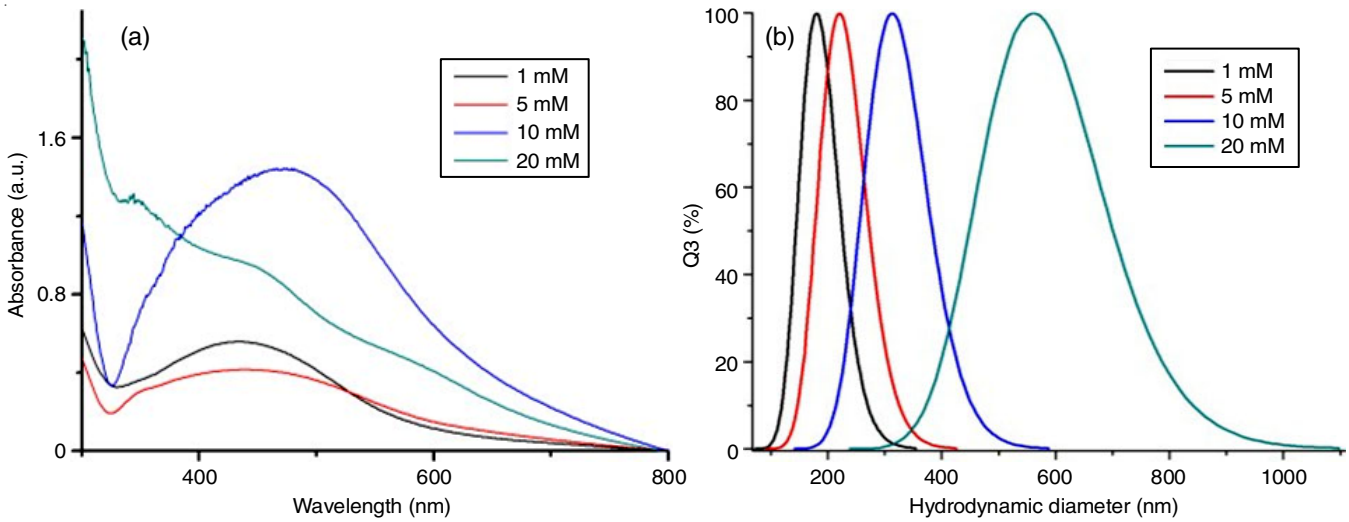

Fig. 4. SPR bands (a) and the size distribution (b) of AgNPs synthesized with varying $AgNO_3$ concentrations (10% plant extract, 100 °C extraction temperature, 3 h incubation time)

starts to diminish. The size of AgNPs is also observed to increase with the increasing concentration of $AgNO_3$ [14].

Study of nucleation and growth processes of AgNPs: According to Fig. 5, the intensity of the SPR peak increases with increasing incubation period indicating an increasing number of AgNPs formed. After 7 h, the intensity shows no obvious increase, indicating the AgNPs synthesis reaction tended towards the equilibrium.

According to the results, it was concluded that the optimum conditions to synthesize AgNPs using *A. glabra* leaf extract are leaf extraction temperature at 100 °C, 10% plant extract, 1 mM $AgNO_3$ solution and 3 h of incubation. Hence, the AgNPs synthesized at these conditions were used in further studies.

Morphological studies: The AgNPs synthesized under optimum conditions were subjected to characterization. The TEM and SEM images of the synthesized AgNPs are shown in Fig. 6. Images show that nanoparticles are mostly spherical in shape and polydispersed. The average size of the nanoparticles according to the TEM images varies between 50-85 nm with lesser quantity of nanoparticles with larger sizes between 110-195 nm.

FT-IR studies: The leaf extract and the synthesized AgNPs show similar peaks in their respective spectra. The prominent peaks were observed for O-H (broad band above 3000 cm^{-1}), C-H (2948 cm^{-1}), C=O (1700 cm^{-1}) and C-O (1300-1100 cm^{-1}) stretching of the biomolecules present in the plant extract (Fig. 7). The peak positions of the two spectra indicate the presence of phenol, alcohol, aldehyde and ketones in the leaf extract and AgNPs [15-17]. These spectra confirm the dual role of leaf extract as reducing and stabilizing agent.

X-ray crystallographic analysis: The X-ray diffraction (XRD) pattern of the synthesized AgNPs (Fig. 8) show peaks at 37.8º, 44.0º, 64.3º and 77.4º corresponding to the (1 1 1), (2 0 0), (2 2 0) and (3 1 1) Bragg reflections of cubic face centered

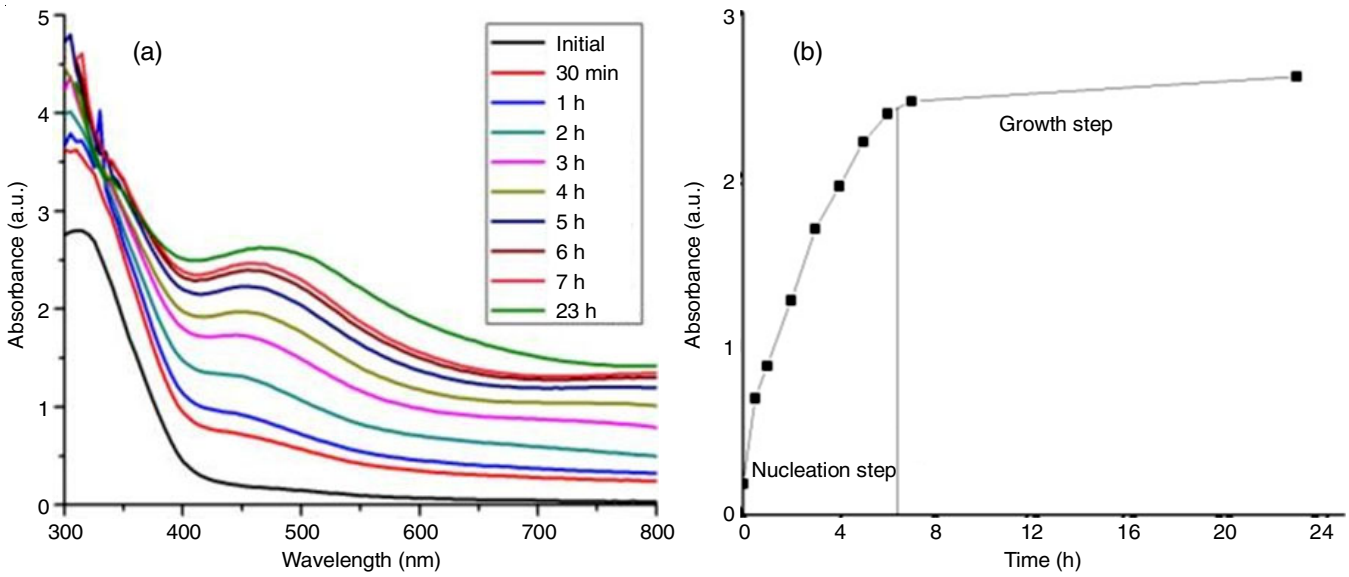

Fig. 5. Absorption spectra (a) and the change of λ_{max} with time (b) of AgNPs in aliquots taken at different time intervals during the course of synthesis for 23 h

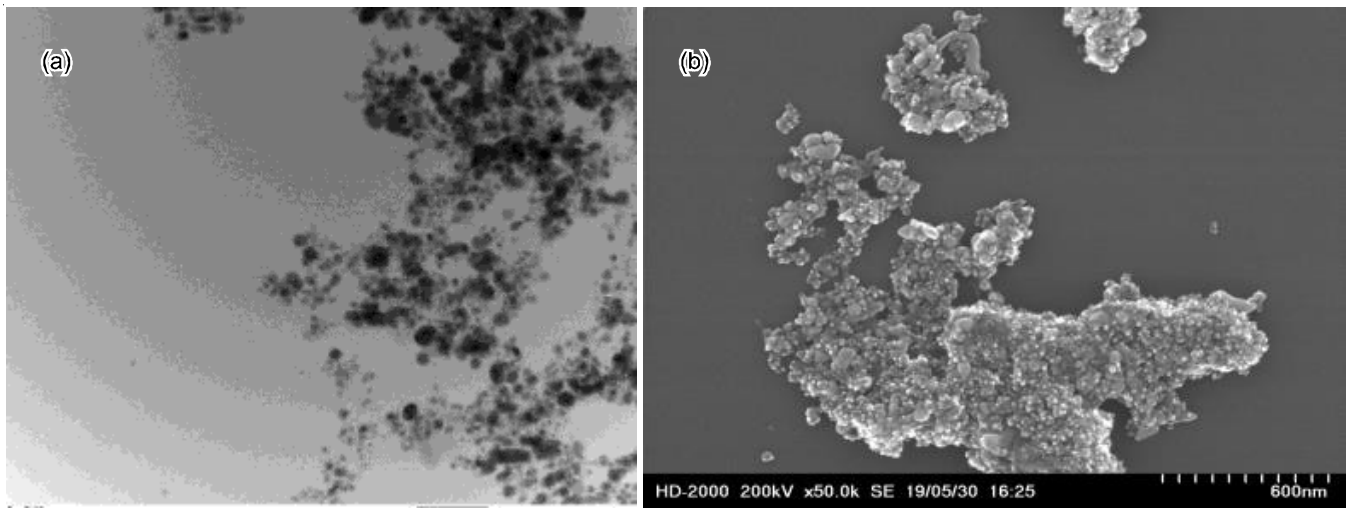

Fig. 6. Electron microscopic images of biosynthesized AgNPs; (a) TEM image, (b) SEM image

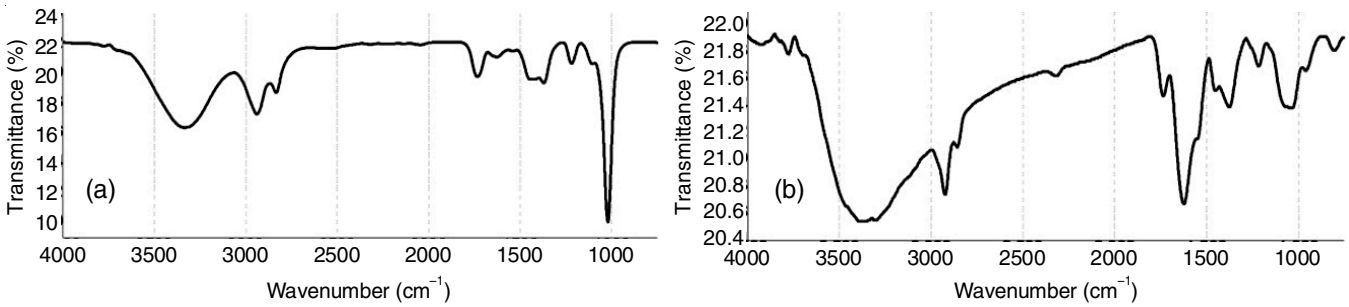

Fig. 7. FT-IR spectra of plant extract (a) and AgNPs (b)

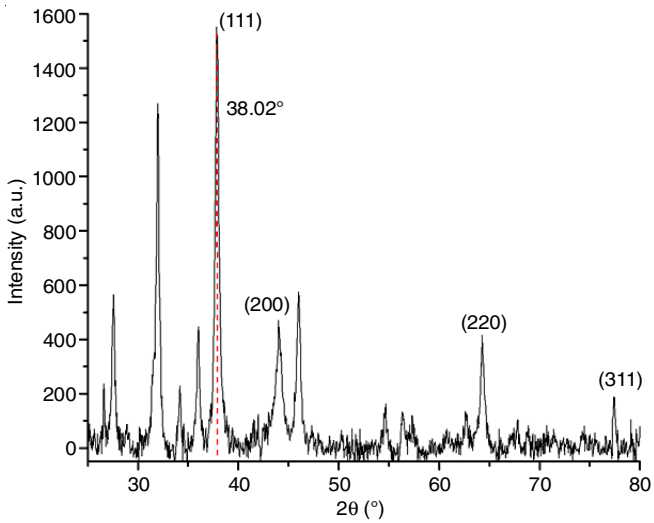

Fig. 8. X-ray diffraction pattern of AgNPs

lattice planes. Calculation of the average particle size using the Debye-Scherrer formula gave a value of 55.4 nm which is in accordance with the size determined by TEM images. The particle size obtained with DLS method is higher than the average particle size obtained from TEM and X-ray diffraction analysis methods. Larger aggregates from the plant extract or AgNP aggregates in the sample could interfere with the DLS measurements. Das *et al.* [18] reported that the difference in particle size distribution in DLS as compared to that observed in TEM analysis could be due to the water absorption on electrostatic stabilized AgNPs.

Photocatalytic activity: Degradation of methylene blue dye was monitored by the change in intensity of the absorption peak of methylene blue at 665 nm. Degradation of methylene blue dye by AgNPs is shown in Fig. 9. The degradation of methylene blue dye by bare AgNPs almost ceases after 2 h. The percentage degradation at the end of 3 h was 19.19%, while after 1.5 h, the test solution became opaque. The Ag^+ ions released from the AgNPs due to the lower stability of nanoparticles could be forming AgCl or Ag_2CO_3 with anions in the medium [19]. However, AgNPs stabilized with Tween-80 show 89.34% reduction in absorption after 3 h (Fig. 9b). This indicates that Tween-80 stabilization has prolonged the shelf life of AgNPs thus improving the photocatalytic activity. This was also visible in the test solution where the solution turned almost colourless after 3 h without possessing an opacity.

Toxic potential of AgNPs on *D. magna*: Different concentrations of AgNPs and Ag^+ ion solutions used in this study exerts different degrees of toxic effects on the swimming capabilities of *D. magna* under otherwise identical test conditions. Toxic effects of AgNPs are mainly due to the release of Ag^+ ions from nanosilver. All toxicity-concentration relationships were based on the measured AgNPs and Ag^+ concentrations in the exposure media. The percentage immobility of the daphnids were found to increase with the increase in tested concentrations of both AgNPs and Ag^+. After 48 h exposure time, 100% immobility

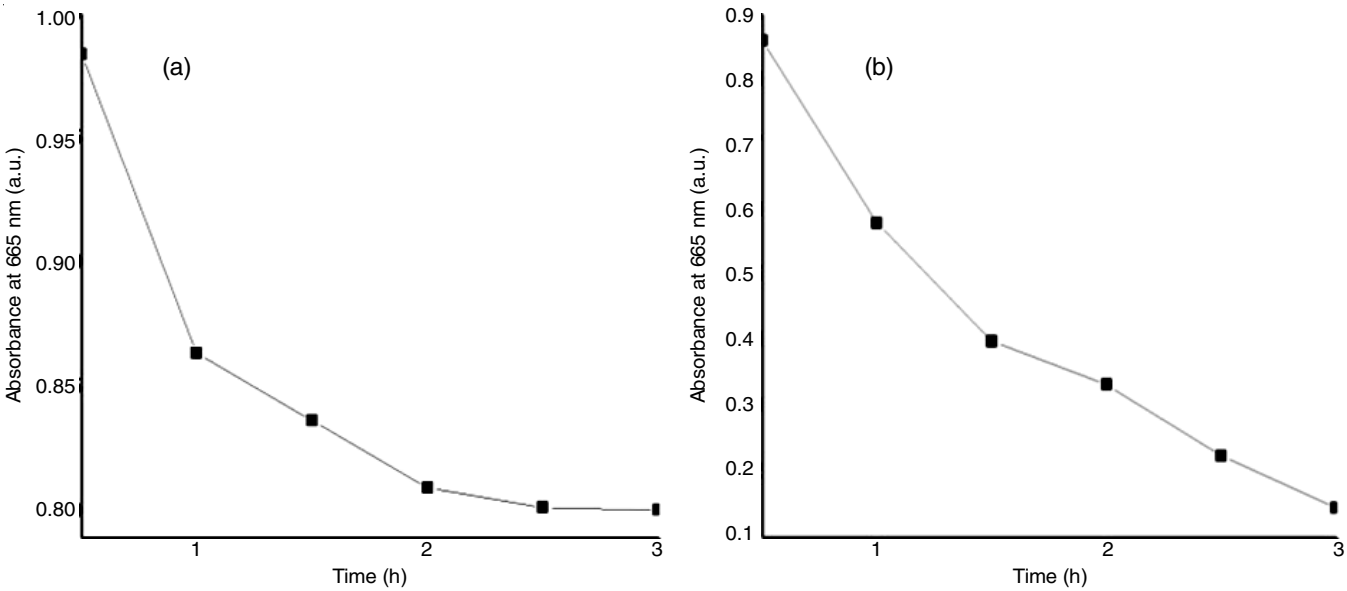

Fig. 9. Degradation of methylene blue by bare (a) and stabilized (b) AgNPs

of daphnids were observed in 2.0, 4.0 and 5.0 mg/L solutions of Ag^+ and AgNPs-stabilized and AgNPs-bare, respectively (Table-4). Both AgNPs and Ag^+ showed a decrease in mobility of *D. magna* with the increased concentrations. Based on the tolerance distribution modelling of the concentration and immobility rate relationships, adverse effect concentrations for 50% immobility percentage (EC_{50}) for *D. magna* after 48 h exposure to AgNPs (bare and stabilized) and Ag^+ were estimated. The EC_{50} values obtained as 3.96 ± 1.1 mg/L and 1.78 ± 0.20 mg/L for bare and stabilized AgNPs, respectively. For Ag^+ ions, it was 1.41 ± 0.2 µg/L. Hence, it is concluded that the biosynthesized AgNPs exert lesser toxicity to *D. magna* than Ag^+ ions. Tween-80 stabilized AgNPs are comparatively more toxic than the bare AgNPs. Tween-80 bring about a steric stabilization effect on the bare AgNPs increasing its lifetime in the test solution. This increases the toxic effects towards the daphnids in the medium. As the stability of bare AgNPs is low, aggregation and precipitation of AgNPs occur lowering the bioavailability of AgNPs in the medium which in turn lowers the EC_{50} value.

TABLE-4
IMMOBILITY PERCENTAGE OF *D. magna* AFTER 48 h FOR BARE AgNPs, STABILIZED AgNPs AND Ag^+ ION SOLUTION

Concentration of Ag^+/AgNPs	Immobility (%)		
	Ag^+	AgNPs (bare)	AgNPs (stabilized)
0.5	7.5	0	0
1.0	25	0	0
1.5	57.5	0	0
2.0	100^a	10^b	12.5^b
3.0	–	25^c	72.5^b
4.0	–	50^c	100^b
5.0	–	100	100

Values followed by common letter(s) are not significantly different ($p > 0.05$) by ANOVA, Dunnett's test n = 3.

Conclusion

The modified method used in this study yielded AgNPs within the nanoscale with optimized conditions of 10% plant extract made by boiling leaves of *Annona glabra* at 100 ºC, 1 mM $AgNO_3$ precursor solution and 3 h of incubation. Surface plasmon resonance peak of the formed AgNPs lies around 419 nm with an average size less than 190 nm. The TEM and SEM images confirmed that the AgNPs are almost spherical in shape and according to these images average size varied between 50-85 nm. The synthesized AgNPs showed the photocatalytic activity against methylene blue dye while more efficient photocatalytic properties could be obtained by stabilizing AgNPs with Tween-80. Moreover, AgNPs exert lesser toxic effects towards *Daphnia magna* than silver ions.

ACKNOWLEDGEMENTS

This work was supported by the University of Kelaniya, research grant RP/03/02/06/02/2019. The authors acknowledge to Mr. Amila Kannangara, Department of Chemistry, University of Kelaniya for providing technical assistance in FTIR analysis.

CONFLICT OF INTEREST

The authors declare that there is no conflict of interests regarding the publication of this article.

REFERENCES

1. L.D. Geoffrion and G. Guisbiers, *J. Phys. Chem. Solids*, **140**, 109320 (2020); https://doi.org/10.1016/j.jpcs.2019.109320
2. J. Jeevanandam, A. Barhoum, Y.S. Chan, A. Dufresne and M.K. Danquah, *Beilstein J. Nanotechnol.*, **9**, 1050 (2018); https://doi.org/10.3762/bjnano.9.98
3. V. Bharathi, J. Firdous, N. Muhamad and R. Mona, *Natl. J. Physiol. Pharm. Pharmacol.*, **7**, 1364 (2017); https://doi.org/10.5455/njppp.2017.7.0725428082017
4. S. Ahmed, M. Ahmad and B.L. Swami, *J. Radiat. Res. Appl. Sci.*, **9**, 1 (2016); https://doi.org/10.1016/j.jrras.2015.06.006
5. L.D. Amarasinghe, P.A.S.R. Wickramarachchi, A.A.A.U. Aberathna, W.S. Sithara and C.R. De Silva, *Heliyon*, **6**, e04322 (2020); https://doi.org/10.1016/j.heliyon.2020.e04322

6. K. Anandalakshmi, J. Venugobal and V. Ramasamy, *Appl. Nanosci.*, **6**, 399 (2016); https://doi.org/10.1007/s13204-015-0449-z
7. Y. He, F. Wei, Z. Ma, H. Zhang, Q. Yang, B. Yao, Z. Huang, J. Li, C. Zeng and Q. Zhang, *RSC Adv.*, **7**, 39842 (2017); https://doi.org/10.1039/C7RA05286C
8. N.R. Panyala, E.M. Peña-Méndez and J. Havel, *J. Appl. Biomed.*, **6**, 117 (2008); https://doi.org/10.32725/jab.2008.015
9. P.V. Asharani, Y. Lian Wu, Z. Gong and S. Valiyaveettil, *Nanotechnology*, **19**, 255102 (2008); https://doi.org/10.1088/0957-4484/19/25/255102
10. S. Lekamge, A.F. Miranda, A. Abraham, V. Li, R. Shukla, V. Bansal and D. Nugegoda, *Front. Environ. Sci.*, **6**, 152 (2018); https://doi.org/10.3389/fenvs.2018.00152
11. M. Vanaja, K. Paulkumar, S. Rajeshkumar, G. Gnanajobitha, M. Baburaja, C. Malarkodi, M. Sivakavinesan and G. Annadurai, *Bioinorg. Chem. Appl.*, **2014**, 742346 (2014); https://doi.org/10.1155/2014/742346
12. OECD, OECD Guidelines for the Testing of Chemicals 202: Daphnia sp., Acute Immobilisation Test and Reproduction Test, OECD (2004).
13. C.B. Cochrane, P.K.R. Nair, S.J. Melnick, C. Ramachandran and A.P. Resek, *Anticancer Res.*, **28(2A)**, 965 (2008).
14. R. Kumar, G. Ghoshal, A. Jain and M. Goyal, *J. Nanomed. Nanotechnol.*, **8**, 452 (2017); https://doi.org/10.4172/2157-7439.1000452
15. M. Govarthanan, M. Cho, J. Park, J. Jang, Y. Yi, S. Kamala-Kannan and B. Oh, *J. Nanomater.*, **2016**, 7412431 (2016); https://doi.org/10.1155/2016/7412431
16. B. Moldovan, V. Sincari, M. Perde-Schrepler and L. David, *Nanomaterials*, **8**, 627 (2018); https://doi.org/10.3390/nano8080627
17. K. Ahmad, H.M. Asif, T. Afzal, M.A. Khan, M. Younus, U. Khurshid, M. Safdar, S. Saifulah, B. Ahmad, A. Sufyan, S.A. Ansari, H.M. Alkahtani and I.A. Ansari, *Front. Chem.*, **11**, 1065986 (2023); https://doi.org/10.3389/fchem.2023.1065986
18. https://www.cabi.org/isc/datasheet/5811#toidentity
19. J. Chen, S. Li, J. Luo, R. Wang and W. Ding, *J. Nanomater.*, **2016**, 7135852 (2016); https://doi.org/10.1155/2016/7135852